

Two-body nonleptonic weak decays of charm and bottom mesons

Faheem Hussain* and Michael D. Scadron

Department of Physics, University of Arizona, Tucson, Arizona 85721

(Received 6 February 1984)

Two-body hadronic pseudoscalar and vector PP , PV , and VV weak decays of charm and bottom mesons are systematically investigated. The πP charm modes are predicted to be of order 2%, in agreement with experiment, and the πP bottom modes are of order 0.5%, consistent with expectation.

I. INTRODUCTION

Although two-body meson nonleptonic branching ratios are measured¹ to be small ($\sim 1\%$) in the charmed sector and are also expected² to be even more minute in the bottom sector, they are nevertheless very important because they reveal the fundamental quark- W^\pm weak dynamics. We review the pseudoscalar (P) and vector (V) charmed-meson decays $D \rightarrow PP, PV, VV$, $F \rightarrow PP, PV, VV$, and bottom-meson decays $B \rightarrow PP, PV, VV$ at this time because (i) the D lifetimes τ_+ , τ_b are presumably more reliable now than when initial estimates were made, (ii) the F rates are now being measured,³ (iii) the B lifetime is now thought to be $\tau_b \approx 1.2 \times 10^{-12}$ sec as recently measured⁴ for the bottom-quark decay, and (iv) the b - c Kobayashi-Maskawa (KM) mixing angle⁵ thus deduced is approximately⁶ $V_{bc} \approx 0.06$. Therefore, we are able to make unambiguous predictions of lifetimes and branching ratios to be compared with the upcoming D -meson data analysis of Mark III, the F decays recently measured at Cornell and DESY, and the soon-to-be-obtained B -meson decay data.

Our analysis will be based upon the standard quark-spectator model, where we specifically follow Ref. 7 and (a) include quark-spectator and color-suppressed spectator graphs, with both scaled down from the usual analyses by a factor of 2 in the amplitude due to the current-current structure of the weak Hamiltonian, (b) include a relative minus sign between these graphs due to the mismatch^{7,8} between Cartesian and $\bar{q}q$ meson states, (c) ignore helicity- (and mass-) suppressed quark-annihilation graphs, (d) ignore mass-suppressed quark-tadpole graphs which gen-

erate⁹ the $\Delta I = \frac{1}{2}$ rule in K decays and appear⁷ to increase the $D_{K\bar{K}}/D_{\pi\pi}$ branching ratio from 1 to ~ 3 , but otherwise affect the D -meson Cabibbo-suppressed decay amplitudes at the 30% level, and (e) ignore the f_+, f_- QCD factors¹⁰ which play an important role in inclusive weak decays but are known¹¹ to give vastly inaccurate branching-ratio predictions for $D_{K\pi}$ decays. More specifically we keep $f_+ = f_- = 1$ and argue that (i) gluons which are exchanged within the same hadron serve to build up the dynamically generated quark mass and will be accounted for in the meson decay constant (taking $f_\pm \neq 1$ would double count this effect) and (ii) gluons exchanged between different hadrons can be ignored because of gluon confinement or neglect of final-state interactions. The net result is quark-spectator graphs which correspond to vector-dominance pole graphs calculated in the time-honored fashion as all orders in the strong interaction and first order in the weak interaction.

In Sec. II we treat the charm sector in the simplified context of $SU(4)$, assuming that it is a good coupling symmetry in the context of the Ademollo-Gatto theorem. First we display the Cabibbo-Glashow-Iliopoulos-Maiani (GIM) weak quark current¹² and stress that vacuum saturation of the corresponding weak Hamiltonian is not an approximation [assuming $SU(4)$ flavor is a good coupling symmetry] but an exact statement of the hadronized version of the quark-spectator graphs, provided one maintains⁷ the factor of $\frac{1}{2}$ arising from the current structure of H_w . Without this factor of $\frac{1}{2}$, it is well understood² that the vacuum-saturated D decay rates are an order of magnitude larger than the observed rates. Tables I and II give

TABLE I. PP charm modes.

Mode	Rate (10^{-14} GeV)	Branching ratio ^a (%)	Experimental rate ^b (10^{-14} GeV)	Experimental branching ratio ^b (%)
$D \rightarrow K^- \pi^+$	2.75	2.0	3.3 ± 1.5	2.4 ± 0.4
$\bar{K}^0 \pi^0$	0.15	0.11	3.0 ± 2.0	2.2 ± 1.1
$\bar{K}^0 \pi^+$	1.22	1.7	1.3 ± 0.5	1.8 ± 0.5
$K^- K^+$	0.38	0.28	0.37 ± 0.19	0.27 ± 0.08
$\bar{K}^0 K^+$	0.38	0.52	0.33 ± 0.23	0.45 ± 0.30
$\pi^- \pi^+$	0.089	0.065	0.11 ± 0.07	0.079 ± 0.038
$\pi^0 \pi^+$	0.095	0.13	< 0.4	< 0.5
$F \rightarrow \eta \pi^+$	1.40	4.1		

^aCentral value of total widths taken from Ref. 1. Also used in Tables II and III.

^bReference 1.

TABLE II. PV charm modes.

Mode	Rate (10^{-14} GeV)	Branching ratio ^a (%)	Experimental rate ^b (10^{-14} GeV)	Experimental branching ratio ^b (%)
$D \rightarrow K^- \rho^+$	3.4	2.5	$9.9^{+4.1}_{-4.3}$	$7.2^{+3.0}_{-3.1}$
$\bar{K}^0 \rho^0$	0.09	0.06	$0.14^{+0.8}_{-0.14}$	$0.1^{+0.6}_{-0.1}$
$\bar{K}^0 \rho^+$	4.9	6.9		13 ± 8 ($\bar{K}^0 \pi^+ \pi^0$)
$K^{*0} \pi^+$	1.3	0.95	4.7 ± 1.9	3.4 ± 1.4
$\bar{K}^{*0} \pi^0$	0.19	0.14	$1.9^{+3.2}_{-1.9}$	$1.4^{+2.3}_{-1.4}$
$\bar{K}^{*0} \pi^+$	3.5	4.8	< 2.7	< 3.7
$F \rightarrow \phi \pi$	1.5	[4.4] ^c		4.4 ^c
$K^{*+} \bar{K}^0$	0.35	1.0		
$\bar{K}^{*0} K^+$	0.33	0.97		
$\rho \eta$	1.9	5.5		

^aSee footnote a, Table I.

^bReference 1.

^cSee Ref. 3.

the various PP, PV, VV predicted and observed decay rates and branching ratios for the D and F mesons. Concerning the $PV K^* \pi, \phi \pi,$ and $VV K^* \rho$ and $\phi \rho$ decays, we follow Ref. 2 and apply the $U(2,2)$ currents¹³ which are known to give good results in most other cases. We depart from Ref. 2 by the above factor of $\frac{1}{2}$ and our values $f_+ = f_- = 1$, and also because we choose the opposite sign for the color-suppressed graph relative to the color-enhanced spectator graph.^{7,8}

Given that most of the charm-meson decay predictions are within the experimental range, in Sec. III the same scheme is applied to bottom-meson B_u, B_d, B_s, B_c two-body PP, PV, VV weak decays. For these decays we work in the context of the $SU(6)$ KM mixing matrix. While the charm $\pi \bar{K}$ branching ratios are of order 2%, the πD branching ratios for bottom decays turn out to be $\sim \frac{1}{2}\%$ as expected. Moreover, the charm-anticharm two-body decay rates of the bottom mesons are a total of $\sim 6\%$, consistent with the total width of all hadronic decays induced by $b \rightarrow c \bar{c} s$ transitions. We summarize our conclusions in Sec. IV, and follow with an appendix giving the relevant decay amplitudes and rate formulas.

II. CHARMED-MESON DECAYS

The basis of our approach begins with the standard Cabibbo-GIM¹² weak $SU(4)$ left-handed quark current [with $\gamma_\mu^L = \gamma_\mu (1 - i\gamma_5)$]

$$j_\mu^w = \bar{u} \gamma_\mu^L (d \cos \theta_C + s \sin \theta_C) + \bar{c} \gamma_\mu^L (-d \sin \theta_C + s \cos \theta_C), \quad (1)$$

combined with the weak Hamiltonian density

$$H_{JJ} = \frac{G_w}{2\sqrt{2}} (j_\mu^w j_\mu^{w\dagger} + j_\mu^{w\dagger} j_\mu^w). \quad (2)$$

Then the color-enhanced spectator graph of Fig. 1(a) is hadronized as depicted in Fig. 1(b) which is identical to the vacuum-saturation mnemonic, say, for $D^0 \rightarrow K^- \pi^+$

with amplitude,

$$\begin{aligned} M_{K^- \pi^+} &= \langle K^- \pi^+ | H_{JJ} | D^0 \rangle \\ &= \frac{G_w}{2\sqrt{2}} \cos^2 \theta_C \langle \pi^+ | J^{1+i2, \mu} | 0 \rangle \langle K^- | J_\mu^{13+i14} | D^0 \rangle \\ &= i \frac{G_w}{2} \cos^2 \theta_C f_\pi (m_D^2 - m_K^2) \\ &\approx i 1.67 \times 10^{-6} \text{ GeV}. \end{aligned} \quad (3)$$

Note our $SU(4)$ -symmetry assumption for the Ademollo-Gatto vector vertex

$$\langle K^- | J_\mu^{13+i14} | D^0 \rangle = (p^D + p^K)_\mu.$$

It is also claimed that vacuum saturation as in (3) is a pole-dominance approximation, especially in context of the bag model. From our pure quark-model viewpoint, however, it is difficult to understand how hadronization of quark-spectator graphs could lead to anything else but vacuum saturation.

Converting (3) to a PP rate as listed in the Appendix, we obtain the $K^- \pi^+$ entry in Table I. Note that the additional factor of $\frac{1}{2}$ in (2) as conventionally defined¹⁴ sets the proper scale for (3) in Table I. Without it, all the entries in Table I would be a factor of ~ 4 too large. This

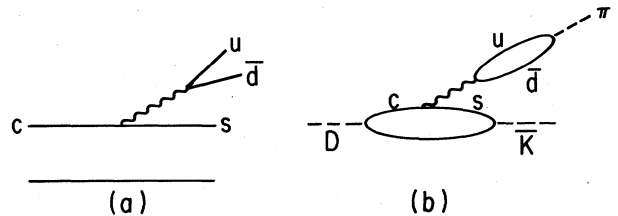


FIG. 1. Quark-spectator graph associated with $c \rightarrow s u \bar{d}$ transitions in Fig. 1(a) and its hadronized version for $D \rightarrow \bar{K} \pi$ in Fig. 1(b).

factor of $\frac{1}{2}$ is missing in Ref. 2 but is critical for the $K^+ \rightarrow \pi^+ \pi^0$ scale of Ref. 9 and the $D_{K\pi}$, $D_{K\bar{K}}$, $D_{\pi\pi}$ scales of Ref. 7. Its origin is that the vacuum-saturation procedure in (2) and (3) picks out the gluon-dressed hadron-current product J^{1+i2}, J^{13+i14} but not J^{13+i14}, J^{1+i2} because the final-state $u\bar{d}$ pion in (3) is a tightly bound (Nambu-Goldstone) boson [signaled by the nonperturbative decay constant f_π in (3)] requiring summing to all orders in the strong interaction. The second (exchange) current product, J^{13+i14}, J^{1+i2} corresponds to the color-suppressed (exchange) spectator graph of Fig. 2 but does not contribute to $D^0 \rightarrow K^- \pi^+$ decay. For the cases of pure leptonic decays or semileptonic decays, the $\bar{1}\bar{v}$ final states are (gluon) free and (2) reduces to the "doubled up" form $H_{JJ} = (G_w/\sqrt{2})j \cdot j^\dagger$. Even for the nonleptonic baryon decays we have an effective doubling up in H_w because both JJ^\dagger and $J^\dagger J$ contribute, with the initial and final baryon states treated as (free) product SU(6) wave functions. In this case vacuum-saturated diagrams play a minor, almost negligible role compared to the much larger W exchange graphs.¹⁵

Another point to notice is that the $D_{\bar{K}^0\pi^+}$ rate due to both the color-enhanced graph of Fig. 1 and the color-suppressed graph of Fig. 2, corresponds to their *difference*⁷ rather than sum, with net amplitude $1 - \frac{1}{3} = \frac{2}{3}$ of the color-enhanced graph. References 2 and 11 add these graphs (and also fold in $f_+ \neq f_-$, whereas we take $f_+ = f_- = 1$). The reason for this sign change is that $\bar{q}q$ quark states which provide a factor of $\frac{1}{3}$ from Fierz reshuffling the color-suppressed diagram must be replaced by Cartesian meson states, e.g.,

$$|\pi^+\rangle = -|1+i2\rangle/\sqrt{2},$$

when computing the vector coupling

$$\langle P^i | V_\mu^j | P^k \rangle = i f^{ijk} (p^i + p^k)_\mu.$$

The net product of these phases is -1 (Refs. 7, 8, and 16), which explains the relative minus sign between color-enhanced and color-suppressed diagrams.

The only $D \rightarrow PP$ rate in Table I which appears to conflict with observation¹ is for $D_{\bar{K}^0\rho^0}$, with large associated errors. We look forward to the Mark III measurements of this mode. Cabibbo-suppressed $D_{K\bar{K}}$ and $D_{\pi\pi}$ rates are also in line with our spectator-model predictions, though in these cases, we must include⁷ 30% corrections due to $\Delta I = \frac{1}{2}$ tadpole graphs (which overwhelmingly dominate the $K_{2\pi}^0$ decays). Only then do we obtain not only all the correct scales, but also the observed branching ratio of $B(D^0 \rightarrow K^- K^+ / \pi^- \pi^+) \sim 4$.

With regard to the PV and VV decay modes, we follow Ref. 2 and employ the U(2,2) prediction¹³ for the axial-



FIG. 2. Color-suppressed quark-spectator graph associated with $c \rightarrow s\bar{d}u$ transitions.

vector current,

$$\langle V^i | A_\mu^j | P^k \rangle = f^{ijk} \epsilon^{*v} [(m_i + m_k) g_{\mu\nu} - 2(m_i + m_k)^{-1} p_\mu^i p_\nu^k] \quad (4)$$

along with

$$\langle 0 | A_\mu^i | P^j \rangle = i f_p \delta^{ij} p_\mu, \quad f_\pi \approx 93 \text{ MeV}, \quad f_K/f_\pi \approx 1.2, \quad (5)$$

and for the vector current,

$$\langle V^i | V_\mu^j | P^k \rangle = -d^{ijk} 2(m_i + m_k)^{-1} \epsilon^{*vi} \epsilon_{\mu\nu\alpha\beta} p_i^\alpha p_k^\beta \quad (6)$$

along with

$$\langle 0 | V_\mu^i | V^j \rangle = f_V m_V^2 \delta^{ij} \epsilon_\mu, \quad f_\rho \approx 0.17. \quad (7)$$

There are two types of PV modes, one of $D^0 \rightarrow K^- \rho^+$ type, with amplitude

$$M_{K^- \rho^+} = \frac{G_w}{2\sqrt{2}} \cos^2 \theta_C \langle \rho^+ | J^{1+i2, \mu} | 0 \rangle \langle K^- | J_\mu^{13+i14} | D^0 \rangle = G_w \cos^2 \theta_C f_\rho m_\rho^2 p^D \cdot \epsilon^*(\rho), \quad (8)$$

and a second of the $D^0 \rightarrow K^{*-} \pi^+$ type, with amplitude

$$M_{K^{*-} \pi^+} = \frac{G_w}{2\sqrt{2}} \cos^2 \theta_C \langle \pi^+ | J^{1+i2, \mu} | 0 \rangle \langle K^{*-} | J_\mu^{13+i14} | D^0 \rangle = -\frac{G_w \cos^2 \theta_C f_\pi}{2(m_D + m_{K^*})} [(m_D + m_{K^*})^2 - 2p^{K^*} \cdot p^\pi] \times p^D \cdot \epsilon^*(K^*). \quad (9)$$

For VV transitions, the $V-A$ current structure of W exchange leads to the typical $D^0 \rightarrow K^{*-} \rho^+$ amplitude

$$M_{K^{*-} \rho^+} = i \frac{G_w \cos^2 \theta_C f_\rho m_\rho^2}{2(m_D + m_{K^*})} \times [(m_D + m_{K^*})^2 g_{\mu\nu} - 2p_\mu^D p_\nu^D - 2\epsilon_{\mu\nu\alpha\beta} p_{K^*}^\alpha p_D^\beta] \times \epsilon^{\mu*}(\rho) \epsilon^{\nu*}(K^*). \quad (10)$$

The only modifications to (8)–(10) that we consider are $\sim 15\%$ from form factors discussed in the Appendix.

The PV results are listed in Table II and the VV results in Table III. The $D^0 \rightarrow K^- \rho^+$, $\bar{K}^0 \rho^0$, and $K^{*-} \pi^+$ rates

TABLE III. VV charm modes.

Mode	Rate (10^{-14} GeV)	Branching ratio ^a (%)
$D \rightarrow K^{*-} \rho^+$	5.4	3.9
$\bar{K}^0 \rho^0$	0.35	0.25
$\bar{K}^0 \rho^+$	2.3	3.2
$F \rightarrow \phi \rho$	5.4	16
$K^{*+} \bar{K}^0$	0.63	1.8

^aSee footnote a, Table I.

are within the range of experiment, although we are suggesting that the $K^-\rho^+$ and $K^{*-}\pi^+$ rates ought to be $\sim \frac{1}{3}$ the scale of the present observed central values. In any event, the large experimental errors do not rule out our predictions yet. The small $\bar{K}^0\rho^0$ rate is more compatible, with the central value about $\frac{1}{40}$ the $K^-\rho^+$ rate due to a color-suppression reduction of 18 and another factor-of-2 suppression coming from the difference between (8) and (9), the latter driving $\bar{K}^0\rho^0$ decay. Nevertheless, the color-suppression factor of 18 is in this data, reconfirming our conviction that it should also suppress the $\bar{K}^0\pi^0$ rate. For the $\bar{K}^0\rho^+$ and $\bar{K}^{*0}\pi^+$ rates, the relative sign of f_ρ and f_π is taken to be positive, as in Eqs. (5) and (7), consistent with the U(2,2) currents.¹³ In Ref. 2 the opposite relative sign was chosen.

Concerning the VV predictions in Table III, they are strikingly large. While the observed $D^0 \rightarrow K^-\pi^+\pi^+\pi^-$ and $D^+ \rightarrow \bar{K}^0\pi^+\pi^+\pi^-$ modes have large branching ratios,¹ the former can only couple to the small $\bar{K}^{*0}\rho^0$ amplitude and the latter cannot couple to VV modes at all.

As for F decays, we assume the ground state is at 1.97 GeV, recently seen by its $F \rightarrow \phi\pi$ decay mode with branching ratio³ 4.4%. The latter is used in Table II to convert the predicted absolute $\phi\pi$ rate to an estimated total F lifetime of $\tau_F \approx 1.9 \times 10^{-12}$ sec. This lifetime is then applied in Table I to estimate the $F \rightarrow \eta\pi$ branching ratio.

III. BOTTOM-MESON DECAYS

The decays of the bottom mesons $B_{\bar{u}} = b\bar{u}$, $B_d^0 = b\bar{d}$, $B_s^0 = b\bar{s}$, and $B_c^- = b\bar{c}$ proceed in much the same manner as charm-meson decays. In the quark diagrams, the relevant transitions are $b \rightarrow c + \bar{u} + d$ and $b \rightarrow c + \bar{c} + s$ in Figs. 3(a) and (b) which are hadronized as in Fig. 1(b). Also in B decays, we add the appropriate color-suppressed diagrams of Fig. 4. Let us note here that the B_c^- decays are dominated by the $c \rightarrow s$ transition because of the KM transition inequality $V_{cs} \gg V_{bc}$.¹⁷ We will discuss this feature of B_c^- decays later in this section.

We employ the same current-current weak Hamiltonian density as defined in (2). However, the presence of a fifth quark flavor modifies the left-handed quark currents which are now defined in terms of the Kobayashi-Maskawa⁵ six-quark model. In this model the current j_μ^w has the form generalized from (1),

$$j_\mu^w = \bar{u}\gamma_\mu^L \tilde{d} + \bar{c}\gamma_\mu^L \tilde{s} + \bar{t}\gamma_\mu^L \tilde{b}. \quad (11)$$

The weak-interaction eigenstates $\tilde{d}, \tilde{s}, \tilde{b}$ are related to the strong-interaction eigenstates d, s, b by

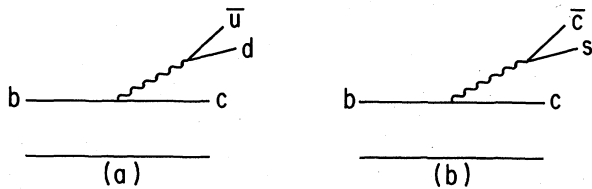


FIG. 3. Quark-spectator graphs associated with $b \rightarrow c\bar{u}d$ transitions in Fig. 3(a), and $b \rightarrow c\bar{c}s$ transitions in Fig. 3(b).

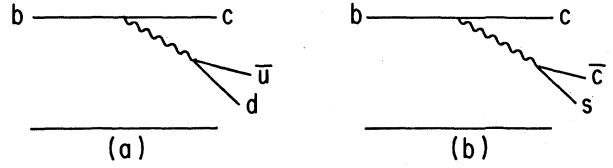


FIG. 4. Color-suppressed quark-spectator graphs associated with $b \rightarrow c\bar{u}d$ transitions in Fig. 4(a) and with $b \rightarrow c\bar{c}s$ transitions in Fig. 4(b).

$$\begin{pmatrix} \tilde{d} \\ \tilde{s} \\ \tilde{b} \end{pmatrix} = V \begin{pmatrix} d \\ s \\ b \end{pmatrix}, \quad (12a)$$

where V is the KM unitary matrix

$$V = \begin{pmatrix} V_{ud} & V_{us} & V_{ub} \\ V_{cd} & V_{cs} & V_{cb} \\ V_{td} & V_{ts} & V_{tb} \end{pmatrix}. \quad (12b)$$

This matrix is consistent with the Cabibbo-GIM current¹ for $V_{ud} \approx \cos\theta_C$, $V_{us} \approx \sin\theta_C$, $V_{cd} \approx -\sin\theta_C$, and $V_{cs} \approx \cos\theta_C$.

For bottom-meson decays, the relevant parameters are V_{ub} and V_{cb} . A recent study¹⁷ estimates the ratio of $b \rightarrow u$ to $b \rightarrow c$ transitions to be $|V_{ub}/V_{cb}| < 0.2$. From a recent measurement of the lifetime⁴ of the bottom quark, $\tau_b \approx 1.2 \times 10^{-12}$ sec, Wolfenstein⁶ has found $V_{bc} \approx 0.06$ based on a calculation of Ginsparg, Glashow, and Wise.¹⁸ The same number is obtained by employing Eq. (2.27) of Ali, Körner, and Kramer.²

An important difference from the D -decay calculations is the estimate of the decay constants f_P and f_V for the charmed pseudoscalar and vector mesons. We follow the same procedure as Ref. 2 with

$$f_V(q_1\bar{q}_2) = \left[\frac{2m_u}{m_{q_1} + m_{q_2}} \right]^{1/2} f_P, \quad (13a)$$

$$f_P(q_1\bar{q}_2) = \left[\frac{m_{q_1} + m_{q_2}}{2m_u} \right]^{1/2} f_\pi. \quad (13b)$$

The PP , PV , and VV rates of the dominant decay modes of the B mesons are listed in Table IV. The masses used in the calculations are

$$m_{B_{u,d}} = 5.27 \text{ GeV}, \quad m_{B_s} = 5.44 \text{ GeV},$$

$$m_{B_c} = 6.43 \text{ GeV},$$

$$m_F = 1.97 \text{ GeV}, \quad m_{F^*} = 2.11 \text{ GeV},$$

$$m_{B_c^*} = 6.57 \text{ GeV}$$

with the quark masses $m_{u,d} = 0.34$ GeV, $m_s = 0.51$ GeV, $m_c = 1.5$ GeV. As Ali, Körner, and Kramer² have noted, the final states involving two heavy charmed mesons are favored despite their smaller phase space. However, the branching ratios for these modes predicted by us are substantially lower than those predicted in Ref. 2. In fact,

TABLE IV. Bottom two-body decay modes (all rates in units of 10^{-14} GeV).

Mode	Branching		Mode	Branching		Mode	Branching	
	PP rate ^a	ratio (%)		PV rate ^a	ratio (%)		VV rate ^a	ratio (%)
$B_d^0 \rightarrow D^+ \pi^-$ $D^+ F^-$	0.20	0.36	$D^{*+} \pi^-$	0.18	0.33	$D^{*+} \rho^-$	0.40	0.73
	0.55	1.00	$D^+ \rho^-$	0.35	0.64	$D^{*+} F^{*-}$	1.61	2.93
			$D^+ F^{*-}$	0.66	1.20			
			$D^{*+} F^-$	0.18	0.33			
$B_u^- \rightarrow D^0 \pi^-$ $D^0 F^-$	0.09	0.16	$D^{*0} \pi^-$	0.26	0.47	$D^{*0} \rho^-$	0.40	0.73
	0.55	1.00	$D^0 \rho^-$	0.39	0.71	$D^{*0} F^{*-}$	1.61	2.93
			$D^{*0} F^-$	0.18	0.33			
			$D^0 F^{*-}$	0.66	1.20			
$B_s^0 \rightarrow F^+ \pi^-$ $F^+ F^-$	0.21	0.38	$F^+ \rho^-$	0.38	0.69	$F^{*+} \rho^-$	0.43	0.78
	0.60	1.09	$F^{*+} \pi^-$	0.20	0.36	$F^{*+} F^{*-}$	1.74	3.17
			$F^+ F^{*-}$	0.75	1.37			
			$F^{*+} F^-$	0.23	0.42			
$B_c^- \rightarrow \eta_c \pi^-$ $\eta_c F^-$ $B_s^0 \pi^-$	0.26		$\eta_c \rho^-$	0.46		$\psi \rho^-$	0.52	
	0.26		$\psi \pi^-$	0.24		ψF^{*-}	0.93	
	3.19		$\eta_c F^{*-}$	0.86				
			ψF^-	0.68				
			$B_s^0 \rho^-$	2.12				
			$B_s^{*0} \pi^-$	1.99				

^a $V_{bc}=0.06$, $\tau_B=1.2 \times 10^{-12}$ sec from Ref. 5.

their total branching ratio for all two-body, double-charm modes of about 20–23% is in contradiction with the expected 10% value for the total hadronic branching ratio that is induced by $b \rightarrow c\bar{c}s$. In contrast, we predict a total branching ratio of $\sim 6\%$ for all two-body, double-charm modes. In general, the predicted rates from Ref. 2 for bottom-meson decays are an order of magnitude larger than expected from general theoretical arguments. It is also well known that there was a similar problem in calculating the branching ratio into two pseudoscalar mesons in charmed-meson decays. All these problems are related to the fact that in previous calculations the crucial factor of $\frac{1}{2}$ had been ignored in the current-current Hamiltonian, Eq. (2), thus overestimating all nonleptonic rates.

Another feature of B -meson decay rates is that the B_c^- two-body decays are dominated by the $B_c^- \rightarrow B_s, B_s^*$ transitions, which are induced by $\bar{c} \rightarrow \bar{s} \bar{u} d$, rather than by the transitions $B_c^- \rightarrow \eta_c, \psi$ in spite of having lower phase space. This is because the $\bar{c} \rightarrow \bar{s} \bar{u} d$ transition comes in with the factor $V_{cs} \simeq \cos\theta_c \simeq 0.974$, which is much larger than $V_{bc} \simeq 0.06$ occurring in $b \rightarrow c\bar{u}d$ transitions.

The rates in Table IV involving π and ρ are likely to be more reliable than the corresponding ones involving F and F^* because of the uncertainty introduced by the absence of experimental data on f_F and f_{F^*} . We have used the specific model (13) to estimate these decay constants and these could be off by large factors.

IV. CONCLUSION

We have attempted to show that the charm- and bottom-meson two-body nonleptonic decays in the quark model have consistent observed and expected branching

ratios and decay rates provided we (a) vacuum-saturate the hadronic amplitudes multiplied by the factor $G_w/2\sqrt{2}$ from the current-current weak Hamiltonian, (b) ignore the QCD factors f_{\pm} in the resulting amplitudes, and (c) choose a relative minus sign between color-enhanced and color-suppressed amplitudes, due to the mismatch between $\bar{q}q$ phases needed at the Fierz-reshuffled weak vertex and the Cartesian factor f^{ijk} occurring at the strong vertex.

Prescriptions (a) and (b) are in fact correlated because nonleptonic amplitudes are nonperturbative in nature and correspond to summing graphs to all orders in the strong (QCD) interaction, but only first order in the weak interaction. The QCD factors f_{\pm} are perturbative in the strong interaction, and the coefficient $G_w/\sqrt{2}$ corresponding to doubling up the currents in leptonic or semi-leptonic transitions is also a perturbative effect because the leptonic currents do not interact strongly. The non-perturbative strong decay constants f_{π}, f_{ρ} , etc., appearing in the vacuum-saturated nonleptonic weak meson amplitudes are signals that perturbative factors such as f_{\pm} and $G_w/\sqrt{2}$ must be altered to $f_{\pm}=1$ and $G_w/2\sqrt{2}$. If the latter factor of $\frac{1}{2}$ is not taken into account, the charmed decay rates are then an order of magnitude larger than experiment and the charm-anticharm two-body decay modes of the bottom meson are themselves greater than the rate into all charm-anticharm modes generated by $b \rightarrow c\bar{c}s$ transitions.

ACKNOWLEDGMENTS

We are grateful for illuminating discussions with R. L. Thews. One of us (F.H.) appreciates the hospitality and

support of the Physics Department, University of Arizona and the travel grant provided by the University Grants Commission, Pakistan. The other author (M.D.S.) acknowledges partial support by the U. S. Department of Energy under Contract No. DE-AC02-80ER10663.

APPENDIX

Kinematic formulas

Labeling our momenta by p_1, p_2, p_3 ($p_1 = p_2 + p_3$) where $1 \rightarrow 2 + 3$, we can express the invariant amplitudes and decay rates as in Ref. 2:

(a) $0^- \rightarrow 0^- + 0^-$

Invariant amplitude:

$$\langle p_2, p_3 | H | p_1 \rangle = M.$$

Decay rate:

$$\Gamma = \frac{p_c}{8\pi m_1^2} |M|^2.$$

(b) $0^- \rightarrow 0^- + 1^-$

Invariant amplitude:

$$\langle p_2, p_3 | H | p_1 \rangle = \epsilon_2^\mu p_{1\mu} M.$$

Decay rate:

$$\begin{aligned} \langle P^i | V_\mu^j | P^k \rangle &= i f^{ijk} [F_+(q^2)(p^i + p^k)_\mu + F_-(q^2)(p^k - p^i)_\mu], \\ \langle V^i | V_\mu^j - A_\mu^j | P^k \rangle &= -f^{ijk} \epsilon^{*\nu} [(m_i + m_k) F_1^A(q^2) g_{\mu\nu} - 2(m_i + m_k)^{-1} F_2^A(q^2) p_\mu^k p_\nu^k] \\ &\quad - d^{ijk} 2(m_i + m_k)^{-1} F_V(q^2) i \epsilon^{*\nu} \epsilon_{\mu\nu\alpha\beta} p^{i\alpha} p^{k\beta}. \end{aligned}$$

Following the Ademollo-Gatto theorem we take $F_- = 0$ throughout. For the other form factors we have taken the canonical forms²

$$F_+ = F_1^A = (1 - q^2/m^2)^{-1}, \quad F_2^A = F_V = (1 - q^2/m^2)^{-2},$$

with m the mass of the appropriate vector or axial-vector meson corresponding to the quantum numbers of the current channel. The axial-vector-meson masses have been taken equal to the corresponding vector-meson masses for the charm and bottom sectors. Inclusion of the U(2,2) prediction for

$$F_- = -(m_k - m_i)/(m_k + m_i)$$

would tend to reduce the predictions of the PP rates only, up to 10% in some cases.

$$\Gamma = \frac{p_c^3}{8\pi m_3^2} |M|^2.$$

(c) $0^- \rightarrow 1^- + 1^-$

Invariant amplitude:

$$\begin{aligned} \langle p_2, p_3 | H | p_1 \rangle &= \epsilon_3^\mu \epsilon_2^{*\nu} (A_1 g_{\mu\nu} + A_2 p_{1\mu} p_{1\nu} \\ &\quad + iB \epsilon_{\mu\nu\alpha\beta} p_1^\alpha p_2^\beta). \end{aligned}$$

Helicity amplitudes:

$$H_{00} = \frac{1}{m_2 m_3} \left[\frac{1}{2} (m_1^2 - m_2^2 - m_3^2) A_1 + m_1^2 p_c^2 A_2 \right],$$

$$H_{--} = A_1 - m_1 p_c B,$$

$$H_{++} = A_1 + m_1 p_c B.$$

Decay rates:

$$\Gamma = \frac{p_c}{8\pi m_1^2} (|H_{00}|^2 + |H_{--}|^2 + |H_{++}|^2).$$

Form factors

The expressions for the current matrix elements in the text have to be modified due to the presence of form factors. We define

*Permanent address: Department of Physics, Quaid-i-Azam University, Islamabad, Pakistan.

¹Particle Data Group, Phys. Lett. **111B**, 1 (1982).

²A. Ali, J. G. Körner, and G. Kramer, Z. Phys. C **1**, 269 (1979).

³A. Chen *et al.*, Phys. Rev. Lett. **51**, 634 (1983).

⁴E. Fernandez *et al.*, Phys. Rev. Lett. **51**, 1022 (1983); N. S. Lockyer *et al.*, *ibid.* **51**, 1316 (1983).

⁵M. Kobayashi and T. Maskawa, Prog. Theor. Phys. **49**, 652 (1973).

⁶L. Wolfenstein, Phys. Rev. Lett. **51**, 1945 (1983).

⁷M. D. Scadron, Phys. Rev. D **29**, 1375 (1984).

⁸G. Eilam, B. H. J. McKellar, and M. D. Scadron, University of Arizona report, 1983 (unpublished).

⁹B. H. J. McKellar and M. D. Scadron, Phys. Rev. D **27**, 157 (1983).

¹⁰M. K. Gaillard and B. W. Lee, Phys. Rev. Lett. **33**, 108 (1974); G. Altarelli and L. Maiani, Phys. Lett. **52B**, 351 (1974).

¹¹N. Cabibbo and L. Maiani, Phys. Rev. Lett. **73B**, 418 (1978); D. Fakirov and B. Stech, Nucl. Phys. **B133**, 315 (1978).

¹²N. Cabibbo, Phys. Rev. Lett. **10**, 531 (1963); S. Glashow, J. Iliopoulos, and L. Maiani, Phys. Rev. D **2**, 1285 (1970).

¹³R. Delbourgo, A. Salam, and J. Strathdee, Proc. R. Soc. London **A278**, 146 (1965).

¹⁴See, e.g., R. E. Marshak, Riazuddin, and C. P. Ryan, *Theory of Weak Interactions in Particle Physics* (Wiley, New York,

- 1969), pp. 566, 567.
- ¹⁵Riazuddin and Fayyazuddin, *Phys. Rev. D* **18**, 1578 (1978); **19**, 1630 (E) (1978); F. Hussain and M. D. Scadron, *Nuovo Cimento* (to be published).
- ¹⁶See, e.g., V. De Alfaro, S. Fubini, G. Furlan, and C. Rossetti, *Currents in Hadron Physics* (North-Holland, Amsterdam, 1973), p. 209.
- ¹⁷B. Gittelman and P. Franzini, in *Proceedings of the 21st International Conference on High Energy Physics, Paris, 1982*, edited by P. Petiau and M. Porneuf [*J. Phys. (Paris) Colloq.* **43**, C3-110 (1982)].
- ¹⁸P. H. Ginsparg, S. L. Glashow, and M. B. Wise, *Phys. Rev. Lett.* **50**, 1415 (1983).